Scripta Materialia 139 (2017) 162–165

Contents lists available at ScienceDirect

Scripta Materialia

journal homepage: www.elsevier.com/locate/scriptamat

Acoustic emissions associated with stress-induced twin boundary mobility in Fe_7Pd_3 ferromagnetic shape memory alloys

A.J. Bischoff[a], S.G. Mayr[a, b, *]

[a] Leibniz Institute of Surface Modification (IOM), Permoserstraße 15, Leipzig 04318, Germany
[b] Division of Surface Physics, University of Leipzig, Linnéstraße 5, Leipzig 04103, Germany

ARTICLE INFO

Article history:
Received 7 May 2017
Received in revised form 14 June 2017
Accepted 15 June 2017
Available online xxxx

Keywords:
Shape memory effect
Twinning dislocations
Acoustic emission
Nanoindentation

ABSTRACT

Twin boundary mobility is an essential prerequisite for the occurrence of magnetic field induced reversible strains in the ferromagnetic shape memory alloy Fe_7Pd_3. To study the behavior of twin boundaries, an abrupt movement of these structures is locally induced by nanoindentation while concomitant acoustic emissions are detected. In martensitic Fe_7Pd_3 bulk sample acoustic emissions can be correlated to pop-in events in the force-depth curves of the nanoindentation indicating twin boundary movement. In contrast, analogous experiments on freestanding Fe_7Pd_3 thin films indicate an insufficient hindering of twin boundary movements within the samples so that no abrupt dislocation displacement bursts take place.

Ferromagnetic shape memory (FSM) alloys are captivating smart functional materials which feature reversible strains of several percent in an applied magnetic field. These macroscopic shape changes are induced by the reorientation of twin variants in the martensitic phase [1] and their magnitude depends essentially on twin boundary mobility, magnetic anisotropy and the axis-ratio of the crystal lattice [2,3]. In this context, the ferromagnetic shape memory alloy Fe_7Pd_3 is of particular interest because of its high ductility, low brittleness [4], and biocompatibility [5] enabling the use of this alloy in miniaturized actuation devices in micromedicine.

The occurrence and magnitude of the FSM effect in a material depend essentially on twin boundary mobility wherefore the behavior of these structures is of particular scientific interest. A possibility to experimentally activate the movement of twin boundaries within a sample is given by nanoindentation. With this technique, a load is applied locally inducing discrete and abrupt events, e.g., stress-induced martensitic transformations or deformation bursts due to reorientation of martensitic variants in shape memory materials as has been investigated for instance in NiTi [6–8] and CuAlBe [9–11]. These so called pop-in or pop-out events are associated with cascade-like shapes of the loading and unloading nanoindentation force-depth curves, respectively. The activated region is thereby spatially limited as shown by finite element modeling of martensitic transformations induced by nanoindentation in NiTi [8]. Here the transformed volume within a sample has a radius of about two times the contact radius of the nanoindenter tip if the indentation takes place in the elastic deformation regime.

In case of martensitic FSM samples, pop-in and pop-out events induced by nanoindentation are expected to originate from abrupt twin boundary movements due to the stress-induced reorientation of martensitic variants. However, cascade-like force-depth curves are also associated with other events such as crack formation, oxide film failure or dislocation nucleation. By additionally analyzing the acoustic emissions correlated with pop-in or pop-out events induced by nanoindentation, both magnitude and type of the triggering event can be identified [12].

In Fe_7Pd_3 thin films, pop-ins have already been observed during nanoindentation [13] but have not yet been studied in detail. In this work, we present nanoindentation experiments performed on Fe_7Pd_3 samples which were placed on a piezo electric acoustic emission sensor. These measurements were conducted to induce locally the movement of twin boundaries within the samples and to use, thus, both force-depth curves and acoustic emission signals to gain a better understanding of twin boundary mobility in FSM alloys. To avoid measurements of stress-induced martensitic transformations, experiments were performed on Fe_7Pd_3 samples in martensitic phase in fct structure. In this particular phase, Fe_7Pd_3 shows both a reversible thermally induced phase transformation to austenite [14]

---

[*] Corresponding author.
E-mail addresses: alina.bischoff@t-online.de (A. Bischoff), stefan.mayr@iom-leipzig.de (S.G. Mayr).

http://dx.doi.org/10.1016/j.scriptamat.2017.06.028
1359-6462/

and a magnetic field induced reorientation of martensitic variants due to the FSM effect [15].

A martensitic Fe_7Pd_3 bulk sample with a composition of $Fe_{71}Pd_{29}$ and a thickness of about 60 μm was fabricated using a splat-quenching technique, as described previously [16]. Therefore, a Fe-Pd ingot with a corresponding composition was prepared by an arc melting procedure and after solidification divided into segments of about 180 mg each. These pieces were then remelted in the arc melter at 600 mbar and splatted between two Cu pistons to ensure rapid solidification. The splat sample exhibited homogeneous surfaces due to polishing with a strong columnar structure and visible surface twinning structures.

Single crystalline Fe_7Pd_3 thin films with a thickness of 500 nm were prepared with molecular beam epitaxy, as basically described previously [17]. The samples were grown from two independently rate-controlled electron beam evaporators with a total rate of 0.15 nm/s on MgO(100) substrates at substrate temperatures of $\approx$ 695 °C. The phase transformation temperature from austenite to martensite of the grown thin films is slightly above room temperature varying a few kelvins due to off-stoichiometry and stresses [18]. Subsequently, the MgO substrates were dissolved in a saturated sodium bicarbonate $NaHCO_3$ solution to obtain freestanding thin films [19]. The used specimens resided in fct-martensitic phase at room temperature as determined with X-ray diffraction (XRD) using a Seifert XRD 3003 PTS. Additionally, the phase of the samples was identified by the distinct degree of tetragonality given by the c/a-axis ratio which was determined with atomic force microscopy (AFM) measurements of the surface relief of the samples using a Veeco Icon Dimension. The thin film specimens showed c/a-ratios of 0.94–0.96, confirming fct-martensitic phase.

Nanoindentation measurements were performed with an ASMEC Universal Nanomechanical Tester device (UNAT) in a classical fast hardness mode according to IOS 14577 using a Berkovich tip of $\approx$ 0.2 μm tip radius. Additionally, measurements on some thin film samples were performed with a dynamical “quasi-continuous-stiffness-measurement” (QCSM) mode [20]. During the loading segment of this mode, a sinusoidal oscillation with a frequency of about 5 Hz is switched on for in total 48 short dwell times of 3 s duration each while the normal force is kept constant. The QCSM mode allows to determine the elastic modulus of the sample depth dependently which is particularly interesting for thin film samples as indenter tip and substrate effects influence the measurement results at small and bigger depths, respectively. Relatively unaffected Young’s moduli are, hence, only obtained in $\approx$ 40–50 nm depth in the case of 500 nm thin films.

For all measurements, samples were placed on top of a Vallen Systeme VS150-M passive piezo electric acoustic emission sensor with a frequency range of 100–450 kHz and a resonance frequency of 150 kHz. The combined measurement set-up is sketched in Fig. 1 and consisted of the acoustic emission sensor, the nanoindenter, a Vallen Systeme AEP3N preamplifier (49 dB gain), a Vallen Systeme DCPL2 signal decoupling box, a National Instruments NI USB 6361 DAQ data acquisition box, a 28 V_{DC} power supply and two computers. Data acquisition of the acoustic emission sensor is controlled with a LabView program and set to an acquisition rate of 150,000 data points/s. Background noise of the sensor amounts to about ± 15 mV. For sample attachment on the sensor the Electron Microscopy Sciences wash-away adhesive Crystalbond 555 was used with a flow point of 54 °C. For a part of the measurements on freestanding thin film samples, moistened films were mounted on the sensor with slight surface drying without using an adhesive. This sample attachment method was mainly used for nanoindentation measurements with the QCSM mode in order to exclude influences of the relatively soft adhesive on the depth dependent Young’s moduli of freestanding Fe_7Pd_3 thin films.

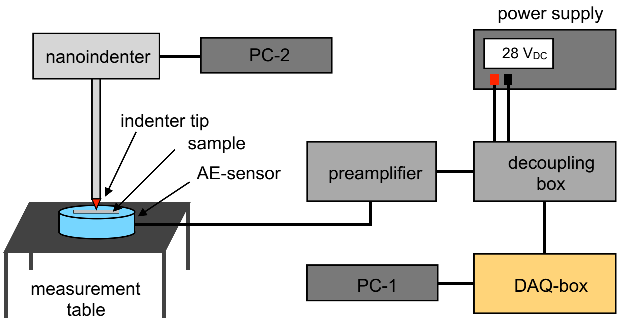

Fig. 1. Sketch of the set-up for the combined nanoindentation and acoustic emission measurements.

Acoustic emission signals were detected during nanoindentation measurements on the martensitic Fe_7Pd_3 splat at chosen maximal indentation forces of 10–100 mN. The loading part of each indentation lasted for 10 s, followed by 1 s creep time and a 4 s unloading segment. At higher maximal indentation forces, stronger acoustic signals were measured as shown in Fig. 2. The individual acoustic signals were associated with weakly defined pop-in events in the corresponding force-depth curves of the nanoindentation measurements.

The relatively low signal levels of both the acoustic and the nanoindentation measurements are caused by the polycrystalline character of the splat. Due to grain boundaries within the sample, more nucleation sources for twinning dislocations are present, however, these boundaries also hinder twin boundary mobility. In the twinned, fct-martensitic splat sample, twin boundary movement is, hence, attenuated resulting in relatively weak measurement signals.

Nanoindentation measurements on freestanding Fe_7Pd_3 thin films were performed at chosen maximal indentation forces of 0.5–5 mN with loading times of 1–10 s. During these measurements no acoustic signals were detected above or below the background noise of the acoustic emission sensor. Moreover, the force-depth curves of the nanoindentation measurements featured hardly ever cascade-like shapes in reasonable indentation depths. Apparently at the investigated force and time scales, twin boundary movement is either not strongly enough hindered within the material to occur in

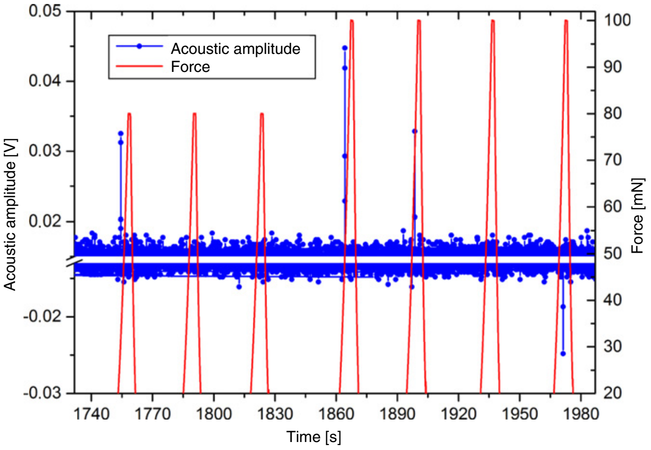

Fig. 2. Acoustic emission signals and force values of the nanoindentation measurement performed on a martensitic Fe_7Pd_3 splat.